Enhanced Rates of Subpicosecond Energy Transfer in Blue-Shifted Light Harvesting LH2 Mutants of *Rhodobacter sphaeroides*†

S. Hess, K. J. Visscher,‡ T. Pullerits, and V. Sundström*

Department of Physical Chemistry, University of Umeå, S-90187 Umeå, Sweden

G. J. S. Fowler and C. N. Hunter

Krebs Institute for Biomolecular Research and Robert Hill Institute for Photosynthesis, University of Sheffield, Sheffield S10 2UH, U.K.

Received January 24, 1994; Revised Manuscript Received April 27, 1994®

ABSTRACT: Energy transfer within various LH2 antenna complexes of the photosynthetic purple bacteria *Rhodobacter sphaeroides* and *Rhodopseudomonas acidophila* has been studied at 77 K using tunable femtosecond and subpicosecond infrared pulses. The complexes examined include the wild-type B800–850 as well as three different specifically mutated complexes. The site-directed mutant strains were altered at positions 44 and 45 near the C-terminus of the α-subunit, which introduces a spectral blue-shift of the 850-nm absorption band. In addition to a constant band at 800 nm, the mutations αTyr44,Tyr45→Phe,Tyr; →Tyr,Phe; and →Phe,Leu have absorption peaks at 838, 838, and 826 nm, respectively. As the spectral overlap between the B800 and the variable bands increases, the rate of energy transfer as measured by the lifetime of the B800 excited state also increases from 2.4 ± 0.2 to 1.8 ± 0.2, 1.6 ± 0.2, and 0.8 ± 0.1 ps. This correlation between energy-transfer rate and spectral blue-shift of the B850 absorption band is in qualitative agreement with the trend predicted from Förster spectral overlap calculations, although the variation of the experimentally determined rate through the series of mutants is somewhat wider than what is predicted by simulations. In addition to the decay time constants related to the B800→B850 energy transfer, the B800 excited state is seen to decay with a faster 150–500-fs component due to energy transfer between spectrally inhomogeneous B800 molecules and possibly also vibrational relaxation and cooling in the bacteriochlorophyll excited state.

The photosynthetic apparatus of the purple photosynthetic bacterium *Rhodobacter* (*Rb.*) *sphaeroides* consists of photochemical reaction centers surrounded and interconnected by light harvesting complexes, which are responsible for increasing the surface area and range of wavelengths over which light energy can be absorbed. The complex that donates energy to the reaction center is the light harvesting antenna 1 (LH1)[1] complex, which absorbs maximally in the near-infrared at approximately 875 nm; it receives energy from the peripheral LH2 complex which has absorption bands at 800 and 850 nm. Bacteriochlorophyll molecules are bound to the α- and β-polypeptides of these LH complexes, and the net result is a large network of interconnecting pigments (Braun & Scherz, 1991; Hunter et al., 1988). The variety of absorbing species in the antenna is a function of several parameters including aggregation to form excitonically coupled dimers, subsequent further aggregation to form larger units, and the proximity to aromatic residues in the C-terminal parts of the α-subunits (Fowler et al., 1992; van Mourik et al., 1990, 1991).

The dynamics of energy transfer within this antenna have been investigated in great detail primarily by measuring the time-resolved absorption transients produced by weak picosecond and, more recently, subpicosecond laser pulses (Zhang et al., 1992; Sundström & van Grondelle, 1992; Shreve et al., 1991; van Grondelle et al., 1987; Sundström et al., 1989). In general, the mode and rate of energy transfer in the antenna are believed to follow the description of Förster for weakly coupled pigments, where the variables include the geometry of the transition dipole moments involved, the center-to-center distance between donor and acceptor transition dipoles (treated as point dipoles), the refractive index of the medium between the pigments, and the overlap integral between the emission spectrum of the donor and the absorbance of the acceptor (Förster, 1948). Despite the importance of the Förster mechanism in photosynthesis, it is difficult to test this theory by varying one of the parameters at a time, especially *in vivo*. However, the recent availability of site-directed LH2 mutants, in which the αTyr44,Tyr45 motif has been replaced by Phe,-Tyr or Phe,Leu, provides an opportunity to test the effect of increasing the spectral overlap on the rate of energy transfer. This arises because the Tyr,Tyr, Phe,Tyr, and Phe,Leu motifs produce absorption bands at 800–850, 800–838, and 800–826 nm, respectively (Fowler et al., 1992). Moreover, there were no rearrangements in the complexes detectable by low-temperature circular and linear dichroism, as well as by fluorescence excitation and emission spectroscopy (Fowler et al., 1992). In this paper, we present the results of studying the energy transfer dynamics within LH2 by monitoring the lifetime of the excited state in the B800 absorption band. We find that as the spectral overlap between the pigments increases

† This work was performed with financial support from The Swedish Natural Science Research Councile and EEC Research Grant SC1*-CT92-0795. G.J.S.F. and C.N.H. gratefully acknowledge financial support from the Agricultural & Food Research Council (AFRC).

* Correspondence should be addressed to this author.

‡ Permanent address: Clinical Chemistry Laboratories, Bornrulaan 34, dg25 DA Leeuwarden, The Netherlands.

® Abstract published in *Advance ACS Abstracts,* June 1, 1994.

[1] Abbreviations: LH1, light harvesting antenna 1; LH2, light harvesting antenna 2; RC, reaction center; Bchl *a*, bacteriochlorophyll *a*; B800, B850, 800- and 850-nm absorbance bands of the LH2 complex; WT, wild type; NIR, near-infrared.

0006-2960/94/0433-8300$04.50/0

in the B800–850, B800–838, and B800–826 complexes, we observe a progressive enhancement of the rate of energy transfer from the B800 pigment, a trend which is qualitatively in agreement with the Förster mechanism.

EXPERIMENTAL PROCEDURES

Mutagenesis of LH2 Genes and Preparation of Membranes. The mutations in the *puc*A gene encoding the α-subunit of the LH2 complex were carried out using the method of Kunkel (Kunkel, 1985; Kunkel et al., 1987), and were verified by DNA sequencing. The altered DNA was cloned into the LH2 expression vector pRKCBC1 and transferred into either the LH2$^-$ LH1$^-$ RC$^-$ *Rb. sphaeroides* recipient DD13/G1 or the LH2$^-$ LH1$^+$ RC$^+$ recipient DBC1 (Jones et al., 1992; Burges et al., 1989). Membranes for spectroscopy were prepared from semiaerobically grown cells, after disruption in a French press and fractionation of the membranes on a 15%/40% w/w sucrose gradient.

Spectroscopy. In order to combine both high temporal and spectral resolution, one-color pump–probe measurements were performed with ~80-fs and ~500-fs tunable infrared pulses. To avoid nonlinear singlet–singlet and singlet–triplet excitation annihilation effects in these highly connected pigment systems, it is absolutely essential to use very low peak and average excitation intensities. The only practical way to achieve this at the moment is in a one-color experiment.

Infrared 450–700-fs dye laser pulses were generated in a cavity-dumped dye laser at 800-kHz–4-MHz repetition rates by pumping it with the compressed and frequency-doubled pulses (~3 ps) of a CW mode-locked Nd^{3+}-YAG laser. The spectral bandwidth of these pulses was ~1 nm. Shorter 60–80-fs pulses were generated in a mode-locked titanium:sapphire (Ti:Sa) laser operating in the range 700–900 nm. The pulse repetition rate of the Ti:Sa laser was reduced from 80 MHz to 800 kHz by an extracavity acousto-optic pulse picker, in order to reduce the average optical power incident on the sample and thereby minimize the buildup of long-lived photoproducts. Before entering the pulse picker, the pulses were stretched in ~2 cm of bulk SF 10 glass in order to prevent damaging of the Bragg cell by the high pulse peak power. After the pulse picker, two SF 10 prisms were used to compress the pulses and to compensate for the wavelength chirp introduced by the pulse picker and pump–probe optics. The autocorrelation function of these pulses, measured at the position of the sample, had an essentially Gaussian time profile and a time–bandwidth product of ~0.46, indicating close to transform-limited chirp-free Gaussian-shaped pulses. Except for the difference in pulsewidth (and thus spectral bandwidth), the experiments with the two different laser systems were equivalent. Kinetics of excited-state decay were measured within the B800 absorption band from 791 to 810 nm. Analysis of the kinetic traces was performed using a least-squares fitting procedure including deconvolution with the measured pulse autocorrelation function. In this way, it was possible to reliably determine time constants of the order of the pulse half-width. A disturbing feature in the one-color pump–probe experiments is the so-called coherent coupling artifact or the coherence spike. This effect is caused by the interference between the two laser beams in the sample, which scatters a small part of the excitation light into the probe beam (Ippen & Shank, 1977). This results in an increased signal amplitude at t = 0 delay time apparent as a spike in the kinetic curve at t = 0, having the width of the pulse autocorrelation function for a well mode-locked pulse (Weiner & Ippen, 1985). With the very short 80-fs pulses, the coherence spike does not present a problem because it is much narrower than the fastest decay components. On the other hand, in the measurements using the ~500-fs dye laser pulses, the pulse (and the coherence spike) is of similar width as the time constants of the B800* decay. Therefore, the kinetics measured with the 500-fs pulses were analyzed in two different ways, with and without subtraction of the coherence spike. Both methods yielded the same trends of the obtained lifetimes, only the absolute values of the lifetimes being somewhat different. The fact that this subtraction procedure yielded significantly better χ^2 values and residuals, and good agreement with the lifetimes obtained with the better time resolution (see Results and Discussion below), makes us confident that this procedure is reliable and does not remove kinetic information of importance. All measurements were performed at 77 K on transparent glasses formed by mixing the membrane solutions with a buffered glycerol/water (3:2) solution to the desired optical density ($A \approx 0.3$/mm). All samples were measured under closed RC (P^+) condition, automatically formed as a result of the high pulse repetition rate which saturates the electron-transfer chain.

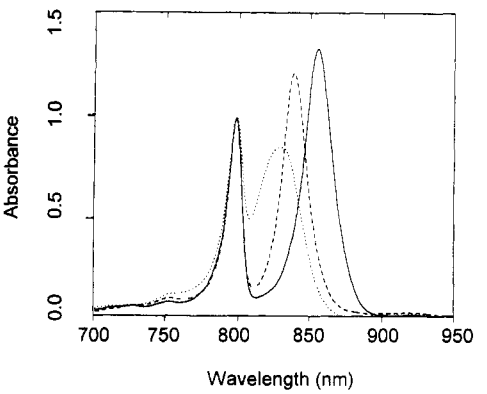

FIGURE 1: 77 K absorption spectra of the wild-type and mutated LH2 antennae of *Rb. sphaeroides*. The LH2 antenna is the only pigment–protein present, which was achieved by expressing wild-type and mutated LH2 genes in a double-deletion (LH2$^-$ LH1$^-$ RC$^-$) background. Solid line, WT; dashed line, αTyr44,Tyr45→Phe,Tyr; dotted line, αTyr44,Tyr45→Phe,Leu.

RESULTS AND DISCUSSION

The rate of energy transfer within the LH2 antenna was studied by measuring the lifetime of the B800 excited state (B800*). The antenna was in its native membrane environment so that detergent-induced artifacts did not complicate the measurements by modifying the wavelength of maximum absorbance of B800 or by changing the aggregation state of the antenna (Kramer et al., 1984; Clayton & Clayton, 1972). The absence of the LH1 and RC complexes was achieved by expressing wild-type and altered LH2 genes in a double-deletion background where the genomic copies of genes for the photosynthetic apparatus have been replaced by antibiotic resistance cassettes. The LH2 antenna is present as a result of the introduction of a plasmid-based LH2 expression system (Fowler et al., 1992; Burges et al., 1989). The LH2-only strains used in this study contained either the wild-type complex or the following mutations at the C-terminus of the α-subunit: αTyr44,Tyr45→Phe,Tyr; αTyr44,Tyr45→Tyr,Phe; or αTyr44,Tyr45→Phe,Leu. The green double-deletion background (LH2$^-$ LH1$^-$ RC$^-$; DD13/G1) is the recipient for these altered LH2 genes (Jones et al., 1992). Low-temperature absorption, CD, and fluorescence polarization data have shown that in each case the progressive shift to the blue (Tyr,-

Table 1: Measured Lifetimes[a] at 800 nm and 77 K with 80-fs Pulses for Wild-Type and Mutant LH2 Complexes of *Rb. sphaeroides*[b]

sample	wavelength (nm)	lifetimes in ps (relative amplitude)		
		τ_f (A_f)	τ_m (A_m)	τ_s (A_s)
Rb. sph. WT (LH2 only)	800	0.4 ± 0.1 (0.45 ± 0.1)	2.4 ± 0.2 (0.55 ± 0.1)	30 ± 5 (–0.5 ± 0.1)
αY44,Y45→FY (LH2 only)	801	0.4 ± 0.1 (0.25 ± 0.05)	1.8 ± 0.2 (0.75 ± 0.05)	20 ± 5 (–0.2 ± 0.05)
αY44,Y45→FL (LH2 only)	800	0.15 ± 0.05 (0.5 ± 0.05)	0.8 ± 0.1 (0.5 ± 0.05)	>30 (–0.3 ± 0.03)
αY44,Y45→FL (LH1+RC)	800	0.15 ± 0.05 (0.3 ± 0.1)	0.7 ± 0.1 (0.7 ± 0.1)	>30 (–0.2 ± 0.05)

[a] The given values are averages of 5–10 independent measurements. [b] Abbreviations: Y = tyrosine; F = phenylalanine; L = leucine.

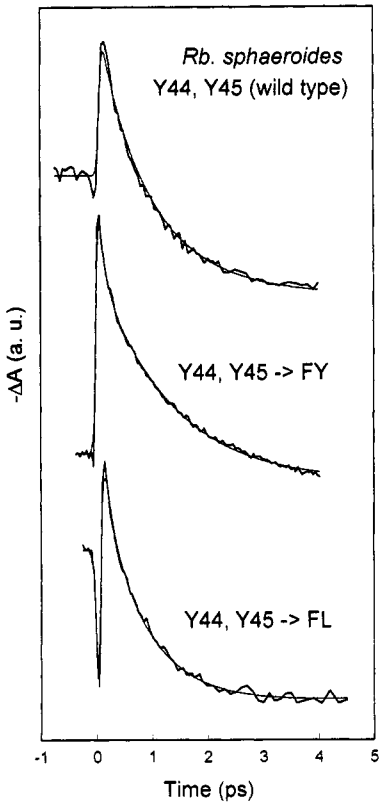

FIGURE 2: Magic-angle decay kinetics of the B800 excited state measured at 77 K with 80-fs pulses for the various LH2 mutants with blue-shifted B850 absorption bands. All measurements are for the LH2-only (double deletion) mutants. *Rb. sphaeroides* WT, 800 nm, τ_f = 0.4 ± 0.1 ps (A_f = 0.45 ± 0.1), τ_m = 2.4 ± 0.2 ps (A_m = 0.55 ± 0.1), τ_s = 30 ± 5 ps (A_s = –0.5 ± 0.1); *Rb. sphaeroides* mutant αTyr44,Tyr45→Phe,Tyr, 801 nm, τ_f = 0.4 ± 0.1 ps (A_f = 0.25 ± 0.05), τ_m = 1.8 ± 0.2 ps (A_m = 0.75 ± 0.05), τ_s = 15 ± 5 ps (A_s = –0.2 ± 0.05); *Rb. sphaeroides* mutant αTyr44,Tyr45→Phe,Leu, 800 nm, τ_f = 0.15 ± 0.05 ps (A_f = 0.5 ± 0.05), τ_m = 0.8 ± 0.1 ps (A_m = 0.5 ± 0.05), $\tau_s \geq$ 30 ps (A_s = –0.3 ± 0.03). See also Table 1 for a summary of the results.

Tyr→Phe,Tyr; Tyr,Phe, 838 nm; Tyr,Tyr→Phe,Leu, 826 nm) has left the 800-nm peak almost unaffected (van Mourik et al., 1990). In order to check that our results were unaffected by the presence of LH1 and RC complexes, genes for these modified LH2 complexes were also expressed in a DBC1 (LH2$^-$ LH1$^+$ RC$^+$) background (Burgess et al., 1989). The absorption spectra in Figure 1 clearly show the effects of mutating the αTyr,Tyr45 motif successively to Phe,Tyr and then Phe,-Leu; a progressive blue-shift of the B850 absorption band is seen.

The kinetics of B800 excited-state decay, as monitored by the absorption recovery measured with 80-fs pulses at 800 nm and 77 K, are shown in Figure 2 (and summarized in Table 1) for *Rb, sphaeroides* WT and Tyr44,Tyr45→Phe,Tyr and Tyr44,Tyr45→Phe,Leu mutants. In all cases, the ground-state bleaching induced by the excitation pulse is seen to decay in a biphasic manner with time constants τ_f = 150–500 fs and τ_m = 0.8–2.5 ps to an increased absorption, which is due to absorption of the B850 (B838, B826) excited-state populated after energy transfer from B800. The sharp negative dip in the signal at t = 0 in some of the traces is due to excited-state absorption from directly optically excited B850. This is evidence by the fact that this rapidly decaying feature is most clearly observed in the αY44,Y45→FL mutant having the most blue-shifted B850 band (B826). In this mutant, the blue wing of the B826 band strongly overlaps with the B800 band, which implies that the dynamics within this part of the B826 band will also be observed for excitation and probing wavelengths within B800. The very fst, ~20 fs, relaxation dynamics of this feature have been studied in detail, and we interpret these very fast processes as relaxation between exciton states of a bacteriochlorophyll aggregate. The details of these results will be presented elsewhere (Pullerits et al., 1994a). The slow decay (τ_s) of B850 excited-state absorption on the ~ 10–200-ps time scale is due to energy equilibration within the B850 pigment pool and trapping by the reaction center. These processes have previously been extensively studied with picosecond time resolution in several wild-type species (Sundström et al., 1986; van Grondelle et al., 1987). The time scale of B800* decay is in agreement with estimates obtained from earlier picosecond measurements at 77 K (van Grondelle et al., 1987; Bergström et al., 1988; Freiberg et al., 1988), but the nonexponential nature of the decay was not observed in measurements with picosecond time resolution. However, in some recent femtosecond measurements on purple bacterial wild-type species (Hess et al., 1994), a similar nonexponentiality was observed at both room temperature and 77 K, and it was concluded that the fastest decay component (τ_f = 150–500 fs) is a result of energy transfer within the inhomogeneously broadened B800 band and/or vibrational relaxation within the B800 excited state. Kinetic measurements at other wavelengths within the 800-nm band with the ~80-fs pulses revealed some wavelength dependence of the amplitudes of the two fastest decay components, the fastest one becoming more intense at shorter wavelengths (Hess et al., 1994), in agreement with the assignment to energy equilibration and/or vibrational relaxation. The broad spectral bandwidth (~15 nm) of these short pulses prevents selective excitation of an inhomogeneously broadened population within a narrow spectral interval, and is therefore expected to yield only a weak variation of relative amplitudes upon tuning of the center wavelength. In order to examine the B800* decay with higher spectral resolution, we also performed the measurements with approximately 500-fs pulses. With this pulse length, the two decay components cannot be resolved, but a weighted average of the two is obtained. The results of these measurements are

Table 2: B800* Lifetimes,[a] Measured with 500-fs Pulses, at Various Wavelengths within the B800 Absorption Band for Wild-Type and Mutant LH2 Complexes[b]

	wavelength monitored for B800* lifetime (lifetime in ps)				
Rb. sph. WT (LH1+RC)		794 (1.9)	797 (2.1)	802 (2.4)	
Rb. sph. WT (LH2 only)	793 (1.9)	795 (1.9)	798 (1.9)	802 (2.2)	
αY44,Y45→FY (LH1+RC)	793 (1.3)		799 (1.6)		806 (1.8)
αY44,Y45→FY (LH2 only)	793 (1.2)	796 (1.4)	800 (1.4)	803 (1.7)	
αY44,Y45→YF (LH2 only)		795 (1.4)	800 (1.4)	802 (1.5)	806 (1.5)
αY44,Y45→FL (LH1+RC)	792 (0.6)	795 (0.7)	799 (0.8)		802 (0.8)
αY44,Y45→FL (LH2 only)	792 (0.7)	795 (0.7)	799 (1.0)	802 (1.1)	803 (1.1)
Rps acid. B800–820 complex			800 (0.7)		804 (1.0)

[a] The given values are averages of several (3–5) independent measurements. The standard deviation of each lifetime is approximately ±10%. [b] Abbreviations: Y = tyrosine; F = phenylalanine; L = leucine.

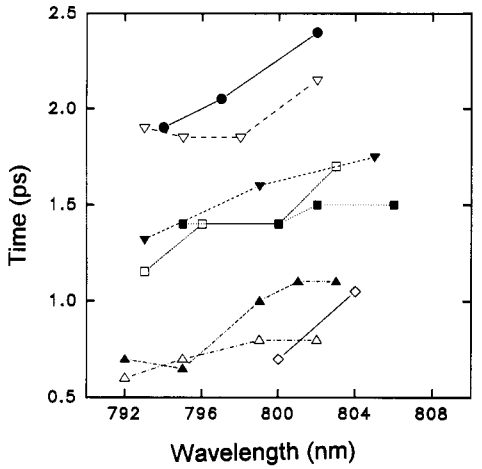

FIGURE 3: Summary of the wavelength dependence of B800* lifetimes as measured with 500-fs pulses: see also Table 2. ● = *Rb. sphaeroides* wild type; ▽ = LH2-only wild-type *Rb. sphaeroides*; □ = αTyr44,Tyr45→Phe,Tyr,LH2 only; ▼ = αTyr44,Tyr45→Phe,Tyr,LH1$^+$,RC$^+$; ■ = αTyr44,Tyr45→Tyr,Phe, LH2 only; ▲ = αTyr44,Tyr45→Phe,Leu, LH2 only; △ = αTyr44,Tyr45→Phe,Leu, LH1$^+$,RC$^+$; ◇ = *Rps. acidophila* B800–820.

summarized in Figure 3 and Table 2, showing a progressive increase of the averaged decay time toward longer wavelengths in the 800-nm band. The lifetimes obtained at the red-most wavelengths for each sample are in very good agreement with the middle component, τ_m = 0.8–2.5 ps, observed in the measurements with the 80-fs pulses (see Figure 2 and Table 1). The combined results of the measurements with femtosecond and subpicosecond pulses thus show that the B800 excited state decays in a (at least) biexponential fashion, due to energy transfer to B850 which occurs with a time constant τ_m of 0.8–2.5 ps, depending on bacterial species and mutant, and due to energy equilibration and/or vibrational relaxation within the B800 excited state taking place with a characteristic time constant of 150–500 fs in the blue wing of the B800 absorption band. In this work where we are mainly addressing the B800→B850 energy-transfer process and its relation to the spectral properties of donor (B800) and acceptor (B850) pigments, we will not further discuss the relaxation processes related to events occurring within the excited state of B800. For a more detailed discussion of these processes, we refer to other recent work (Hess et al., 1994).

We now turn to a discussion of the variation of the B800→B850 energy-transfer rate in the various LH2 complexes, as given by the decay time constant τ_m (see Table 1 and Figure 2) or the lifetime measured with 500-fs pulses in the red wing of the 800-nm band (see Figure 3 and Table 2). The B800→B850 transfer times found for wild-type *Rb. sphaeroides* B800–850 of 2.4 ps and for *Rps. acidophila* B800–820 of 1.0 ps agree very well with the estimates made from earlier measurements performed with longer pulses which suggested a ~2-ps lifetime for B800* in WT LH2 (van Grondelle et al., 1987; Freiberg et al., 1988) and a 1–2-ps lifetime for *Rps. acidophila* B800–820 (Bergström et al., 1988). The 2.4-ps lifetime for *Rb. sphaeroides* also agrees well with the hole-burning data (Reddy et al., 1991; van der Laan et al., 1990) and recent pump–probe experiments using subpicosecond excitation (Visscher et al., 1993, unpublished results). The *Rb. sphaeroides* WT and *Rps. acidophila* B800–820 complex were incorporated in the present work to serve as limiting values for what might be expected for the *Rb. sphaeroides* mutants studied in this paper. As pointed out in the introduction, the series of mutants originates from the *Rb. sphaeroides* wild-type, and by successive site-specific mutagenesis a "*Rps. acidophila*-like" B800–820 mutant was finally obtained (αTyr44,Tyr45→Phe,Leu).

Comparing the B800→B850 energy-transfer times found for the mutations in double-(DD13/G1) and single-deletion (DBC1) backgrounds, we conclude that conducting the measurements on LH2 in the presence of the LH1 antenna and RC's does not influence the rate of the energy transfer significantly, thus supporting the hypothesis that the kinetics around 800 nm mainly reflect internal energy transfer within the LH2 complex. The small differences in measured lifetimes for the various mutants in single- (DBC1) and double-deletion (DD13/G1) backgrounds suggested by Figure 3 lie within experimental error of the measurements with the relatively long 500-fs pulses. The single- and double-deletion mutants of αTyr44,Tyr45→Phe,Leu, displaying the largest difference in the B800 excited-state lifetime in Figure 3, have virtually identical τ_m lifetimes when measured with higher precision using 80-fs pulses (see Table 1). The results compiled in Table 2 also show that the *Rb. sphaeroides* WT and the LH2-only WT have very similar lifetimes. It is clear too that the *Rb. sphaeroides* αTyr44,Tyr45→Phe,Leu mutant, which most resembles the *Rps. acidophila* B800–820 LH2, also has a lifetime comparable to the *Rps. acidophila* complex. The *Rb. sphaeroides* mutants with either one of the αTyr44,Tyr45 residues substituted by a phenylalanine have equal lifetimes which lie between those found for the native B800–850 and B800–820 complexes for *Rb. sphaeroides* and *Rps. acidophila*, respectively. The steady-state absorption spectra for the antennae follow a similar pattern (see Figure 1); the wild-type LH2 of *Rb. sphaeroides* has NIR absorption bands at 800 and 850 nm, both the αTyr44,Tyr45→Phe,Leu mutant and the *Rps. acidophila* complex have bands at 800 and ~820 nm, and all the single tyrosine mutants have NIR bands at 800 and 838 nm. In other words, it seems that the spectral properties govern the energy-transfer process in these species.

We now proceed with an analysis of the B800→B850 energy transfer in terms of the Förster weak coupling mechanism

(Förster, 1948). In the Förster description of the energy-transfer process, the spectral properties of the acceptor and donor molecule play an important role. In the following, we will try to quantify this dependence.

Comparison of the Measured B800→B850 Energy-Transfer Rates with Corresponding Förster Overlap Integrals. According to the Förster theory, the incoherent excitation transfer rate is proportional to the overlap integral of the emission spectrum of the donor, $f_D(\nu)$, and the absorption spectrum of the acceptor, $\epsilon_A(\nu)$:

$$k_{et} = C\int f_D(\nu)\epsilon_A(\nu)\,d\nu \qquad (1)$$

where C does not depend on the energy (strictly speaking, C is not independent of ν, but we ignore this weak dependence in our qualitative calculations).

Due to the short excited-state lifetime of B800, the fluorescence spectrum $f_D(\nu)$ is not very accurately measurable. Furthermore, it would not be correct to use directly measured spectra because of the inhomogeneous broadening—in eq 1, the homogeneous spectra must be used. Therefore, we have carried out the spectral simulations of the B800 and B850 bands of the B800–B850 complex using the model developed in Pullerits et al. (1994b). This model uses the linear harmonic Franck–Condon approximation and enables the calculation of the spectrum of the electronic transition which is coupled to vibronic modes and lattice phonons. We have made use of the vibronic frequencies and relative transition intensities of Bchl *a* reported in Renge et al. (1987). Unfortunately, this work does not give values for the Franck–Condon factors, and we have varied these parameters within reasonable limits to get the fit to experimental spectra. In order to compare the model spectra with experiment, the calculated homogeneous spectra were convoluted with the inhomogeneous distribution function (IDF). The widths of the IDFs of B800 and B850 are taken to be 170 and 60 cm^{-1}, respectively (Reddy et al., 1991). The experimental and calculated absorption spectra of the B800–850 complexes at 150 K are given in the inset of Figure 4. It should be noted that according to Reddy et al. (1991), B850 is mainly homogeneously broadened with the width of 210 cm^{-1} which corresponds to the exciton bandwidth. Our simulations do not take into account the so-called Franck–Condon narrowing of the exciton vibronic bands reported in Reddy et al. (1992). On the other hand, at 77 K all bands are quite broad anyway, and this effect does not affect significantly the overlap integral which depends much more on the overall Franck–Condon factor of the certain spectral region than the width of the lines in this region. In the calculations of the overlap integral, we have assumed that the homogeneous absorption and fluorescence spectra are mirror-symmetric with respect to the 0–0 transition frequency.

We have calculated the dependence of the spectral overlap on the 0–0 transition position of the B850 homogeneous spectrum. The 0–0 transition of the B800 emission was positioned at 800 nm. The reciprocal of the overlap is given in Figure 4 normalized in the way that it at 838 nm coincides with the experimentally determined 1.8-ps transfer time in the mutant αY44,Y45→FY. The curve calculated by the Föster expression qualitatively describes the experimentally determined trend, though the measured dependence seems to be stronger than the simulation predicts.

One possible reason for this discrepancy may be that in the calculation it is assumed that the transfer occurs from a thermally equilibrated donor (B800) excited state. However, in a recent work (Chachisvilis et al., 1994), it was found that

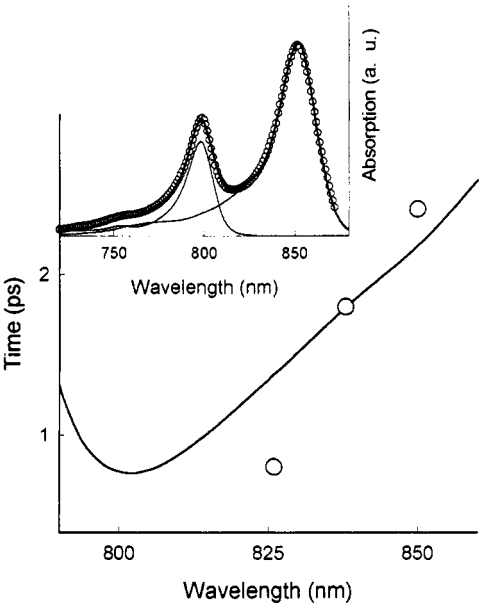

FIGURE 4: Dependence of the B800→B850 energy-transfer time at 77 K on the position of the B850 band. Circles represent the experimentally estimated time constants. The calculated dependence (solid line) is normalized to 1.8 ps at 838 nm. The inset gives the absorption spectrum of the *Rb. sphaeroides* WT B800–850 complexes at 150 K (circles) together with the simulated B800 and B850 spectra (solid lines).

coherent nuclear motions in the excited states of antenna pigment–protein complexes are dephased on the time scale close to the transfer times measured in the present work. This means that the transfer may easily take place from a vibrationally hot state (Tehver & Hizhnyakov, 1976) which obviously would lead to deviations from the calculated rates. We have also used the same homogeneous spectrum for all wavelengths and have neglected any possible variations in electron–phonon coupling and IDF parameters through the series of mutants, which, if present, will change the spectral overlap. It holds in particular for the most blue-shifted mutant which has a significantly broader B850 absorption band than the other two (see Figure 1). Finally, we point out that we cannot exclude the possibility that mutation also changes, besides the spectral properties, the mutual orientation and distances between the pigments which could noticeably affect the transfer rates.

At this point, it is appropriate to discuss and compare our results on B800→B850 energy transfer in the series of LH2 mutants of *Rb. sphaeroides* with some very recent spectral hole-burning results for the same mutants (van der Laan et al., 1993). These measurements were performed at very low temperature (1.6–4 K), and the measured hole widths were related to the B800→B850 energy-transfer rate. The hole-burning results were found to be different in two respects, from those of the present time-resolved experiments. First, except for the wild-type species, where very good agreement between the two methods was observed, the B800* lifetimes of the mutants were found to be longer in the hole-burning study as compared with the time-resolved measurements. Second, the B800→B850 transfer rate as measured in the hole-burning study was not found to increase progressively with increasing spectral blue-shift of the 850-nm band, as observed at 77 K in the time-resolved measurements. Rather, the energy-transfer rate in the series of mutants was only somewhat faster than in the WT species and more or less constant without a clear trend of variation. The hole-burning results were correlated to Förster calculations of energy-

transfer rate based on simulated Gaussian homogeneous spectral bands, and it was concluded that in order to reproduce the weak variation of transfer rate, $(2.5\ ps)^{-1} \rightarrow (\sim 1.8\ ps)^{-1}$, through the mutant series, spectral overlap between B800 fluorescence and a vibronic structure of B850 must be invoked; consideration of only Gaussian-shaped 0–0 electronic transitions would, in disagreement with the experiments, result in a variation of transfer rates over many orders of magnitude. Earlier hole-burning measurements of B800→B850 energy transfer in *Rb. sphaeroides* WT by Reddy et al. (1991, 1992) were given a similar interpretation. In our simulations of the overlap integral, we are using the calculated homogeneous spectra where the vibrational modes of the relevant spectral region are included, and thus the transitions through the vibronic sublevels are taken into account. We have carried out the calculations for 4 K as well, and in accord with the hole-burning results, we found a much weaker dependence of the calculated transfer rate on the position of the maximum of the B850 band in the region above 820 nm than we found at 77 K. Below 820 nm, the 0–0 line together with the corresponding phonon wing is starting to overlap strongly with the broad B850 homogeneous absorption, and the calculated transfer rate starts to increase rapidly. At higher temperatures, when bands are broadened due to the electron–phonon interaction and the fast dephasing of the 0–0 line, this enhanced overlap is working already around 850 nm. This also explains the increase of the B800→B850 transfer rate from $(2.4\ ps)^{-1}$ at 77 K (and 4K) to $(0.6\ ps)^{-1}$ at room temperature observed in the WT B800–850 complexes. According to this model, the blue-shifted mutants are predicted to have a temperature-induced increase of the B800→B850 transfer rate which is switched on at lower temperatures than in the WT complexes where it happens above 77 K. Thus, the results of hole burning at ~4 K and the present time-resolved study are not in conflict, but merely reflect the different parameters that dominate energy transfer at these temperatures.

It should be noted that not only the dipole–dipole interaction considered by Förster but also dipole–quadrupole, quadrupole–quadrupole, and exchange interactions incorporated into the incoherent excitation transfer picture by Dexter (1953) lead to a linear dependence of the transfer rate on the spectral overlap. However, these interactions have a very short range and are quite unlikely to be significant in our case.

We conclude that these blue-shifted antenna mutants have provided a good model system in which to examine predictions arising from the Förster incoherent energy-transfer theory, and that the progressive spectral overlap is reasonably consistent with the observed transfer rates.

REFERENCES

Bergström, H., Sundström, V., van Grondelle, R., Gillbro, T., & Cogdell, R. J. (1988) *Biochim. Biophys. Acta 936*, 90.

Braun, P., & Scherz, A. (1991) *Biochemistry 30*, 5177.

Burgess, J. G., Ashby, M. K., & Hunter, C. N. (1989) *J. Gen. Microbiol. 135*, 1809.

Chachisvilis, M., Pullerits, T., Jones, M. R., Hunter, C. N., & Sundström, V. (1994) *Chem. Phys. Lett.* (in press).

Clayton, R. K., & Clayton, B. J. (1972) *Biochim. Biophys. Acta 283*, 492.

Dexter, D. L. (1953) *J. Chem. Phys. 21*, 836.

Förster, Th. (1948) *Ann. Phys. 2*, 55.

Fowler, G. J. S., Visschers, R. W., Grief, G. G., van Grondelle, R., & Hunter, C. N. (1992) *Nature 355*, 848.

Freiberg, A., Godik, V. I., Pullerits, T., & Timpmann, K. (1988) *Chem. Phys. 128*, 227.

Hess, S., Feldshtein, F., Babin, A., Nurgaleev, I., Pullerits, T., Sergeev, A., & Sundström, V. (1993) *Chem. Phys. Lett. 216*, 247.

Hunter, C. N., Pennoyer, J. D., Sturgis, J. N., Farrelly, D., & Niederman, R. A. (1988) *Biochemistry 27*, 3459.

Ippen, E. P., & Shank, C. V. (1977) *Top. Appl. Phys. 18*, 83–122.

Jones, M. R., Fowler, G. J. S., Gibson, L. C. D., Grief, G. G., Olsen, J. D., Crielard, W., & Hunter, C. N. (1992) *Mol. Microbiol. 6*, 1173.

Kramer, H. J. M., van Grondelle, R., Hunter, C. N., Westerhuis, W. H. J., & Amesz, J. (1984) *Biochim. Biophys. Acta 765*, 156.

Kunkel, T. A. (1985) *Proc. Natl. Acad. Sci. U.S.A. 82*, 488.

Kunkel, T. A., Roberts, J. D., & Zakour, R. A. (1987) *Methods Enzymol. 154*, 367.

Pullerits, T., Chachisvilis, M., Jones, M. R., Hunter, C. N., & Sundström, V. (1994a) *Chem. Phys. Lett.* (in press).

Pullerits, T., van Mourik, F., Monshouwer, R., Visschers, R. W., & van Grondelle, R. (1994b) *J. Lumin. 58*, 168.

Reddy, N. R. S., Small, G. J., Seibert, M., & Picorel, R. (1991) *Chem. Phys. Lett. 181*, 391.

Reddy, N. R. S., Picorel, R., & Small, G. J. (1992) *J. Phys. Chem. 96*, 6458.

Renge, I., Mauring, K., & Avarmaa, R. (1987) *J. Lumin. 37*, 207.

Shreve, A. P., Trautmann, J. K., Frank, H. A., Owens, T. G., & Albrecht, A. C. (1991) *Biochim. Biophys. Acta 1058*, 280.

Sundström, V., & van Grondelle, R. (1992) *J. Photochem. Photobiol. 15*, 141.

Sundström, V., van Grondelle, R., Bergström, H., Akesson, E., & Gillbro, T. (1986) *Biochim. Biophys. Acta 851*, 431.

Tehver, I., & Hizhnyakov, V. (1976) *Sov. Phys.—JETP 42*, 305.

van der Laan, H., Schmidt, Th., Visschers, R. W., Visscher, K. J., van Grondelle, R., & Völker, S. (1990) *Chem. Phys. Lett. 170*, 231.

van der Laan, H., De Caro, C., Schmidt, Th., Visschers, R. W., van Grondelle, R., Fowler, G. J. S., Hunter, C. N., & Völker, S. (1993) *Chem. Phys. Lett. 212*, 569.

van Grondelle, R., Bergström, H., Sundström, V., & Gillbro, T. (1987) *Biochim. Biophys. Acta 894*, 313.

van Mourik, F., Visschers, R. W., Chang, M. C., Cogdell, R. J., Sundström, V., & van Grondelle, R. (1990) in *Molecular Biology of Membrane-Bound Complexes in Photosynthetic Bacteria* (Drews, G., & Dawes, E. A., Eds.) pp 345–356, Plenum Press, New York.

van Mourik, F., van der Oord, C. J. R., Visscher, K. J., Parkes-Loach, P. S., Loach, P. A., Visschers, R. W., & van Grondelle, R. (1991) *Biochim. Biophys. Acta 1059*, 111.

Weiner, A. M., & Ippen, E. P. (1985) *Chem. Phys. Lett. 114*, 456.

Zhang, F. G., van Grondelle, R., & Sundström, V. (1992) *Biophys. J. 61*, 911.